ROMANIAN JOURNAL OF INFORMATION SCIENCE AND TECHNOLOGY
Volume 27, Number 3–4, 2024, 348–361

Stable Levitation of Single-point Levitation Systems for Maglev Trains by Improved Cascade Control

Jie WEN[1, *] and Fangling WANG[2]

[1]School of Electrical and Control Engineering, North University of China, Taiyuan, 030051, China
[2]School of Mechanical Engineering, North University of China, Taiyuan 030051, China
Email: wenjie015@gmail.com*, junxinkeqing07@outlook.com
* Corresponding author

Abstract. The stable levitation of single-point levitation systems for electromagnetic suspension (EMS) maglev trains, which belongs to the control task of nonlinear and unstable systems, is investigated in this paper. Considering the simplicity and convenience of the control application, we dedicate ourselves to combining and applying common control methods to achieve the stable levitation rather than designing complex controls or using advanced control methods. For this goal, the single-point levitation system is divided into an electromagnetic system and a motion system first. On this basis, we design the Lyapunov controller and sliding mode controller as Controller I, while another Lyapunov controller and the standard Proportional Integral Derivative (PID) controller are designed as Controller II, which are used to control the electromagnetic system and motion system respectively and constitute the improved cascade control to achieve the stable levitation. Furthermore, the switching controller consisting of the standard PID controller and the designed Lyapunov controller is used as Controller II for the improvement of both stability and robustness.

Key-words: Single-point levitation systems; maglev train; sliding mode control; Lyapunov control; cascade control.

1. Introduction

In recent years, travel has always been one of the top priorities in people's lives. However, due to the friction and vibration between the train and the track, the running comfort and speed of the train are greatly affected. Maglev trains rely on electromagnetic suction or electromagnetic repulsion to levitate and guide the train on the track, achieving no mechanical contact between the train and the ground track, then use linear motors to drive the train. Since there is no mechanical contact between the train and the track during traction operation, the wheel-rail adhesion

limitation, mechanical noise as well as the wear and tear of traditional trains can be overcome, so that maglev trains becomes a new type of transportation tool.

The levitation system of maglev trains is a complex nonlinear system with open-loop instability, susceptibility to interference, strong coupling, etc. The traditional methods of designing controllers for maglev systems are based on local linearization near the equilibrium point of the controlled system to design the controllers by applying the approaches for linear systems [1]. For examples, the model-free adaptive control method based on full-format dynamic linearization was applied to a single-degree-of-freedom magnetically levitated system in [2]. Wai and Lee designed a robust fuzzy-neural-network control scheme for the levitated positioning of the linear maglev rail system with nonnegative inputs [3]. Recently, based on the theory of linear active disturbance rejection control and generalized predictive control, Wang et al. designed a levitation controller to obtain better tracking and robustness for the levitation system of maglev trains after the equilibrium point was linearized [4].

However, when the magnetic levitation system works under the conditions of a wide range of bearing capacity and working air gap variation, the controller based on the optimization of the equilibrium point parameters is not easy to obtain the ideal control effect. Various nonlinear control methods, e.g., backstepping control [5], sliding mode control [6, 7], robust control [8], have been used to overcome the above problems. For example, Sun et al. designed a fuzzy sliding mode controller to handle the disturbance, nonlinear and parameter perturbation to improve the dynamic performance [9]. Further, an adaptive neural-fuzzy sliding mode controller was proposed to reject the disturbance and parameter perturbations for the magnetic suspension system of a low-speed maglev train [6], while an amplitude saturation controller is proposed and improved based on radial basis function neural networks for the EMS maglev train [10]. Based on the sliding mode control, Chen et al. combined an acceleration feedback correction module and an adaptive compensation loop to deal with the time-varying disturbance of non-uniformity and load for maglev train suspension system [7]. Moreover, for the better stability and comfort of high-speed maglev operation on inhomogeneous tracks, Jiang et al. proposed a robust control method by combining a fixed time perturbation observer and a global finite-time controller [8]. In particular, with the vigorous development of artificial intelligence technology, deep learning [11], reinforcement learning [12] have also been applied to the levitation control of maglev trains.

Instead of local linearization, the stable levitation of nonlinear maglev systems, which is regarded as a complex control problem, is studied directly in this paper. Considering the practicality and realizability of the controller, the main idea of accomplishing the control tasks of complex nonlinear systems in this paper is to apply, pair or combine simple and common control methods rather than design complex controls or apply advanced control methods. According to this idea, we dedicate to the combination and collocation of simple control methods to achieve the stable levitation of nonlinear magnetic levitation systems in this paper. Considering that the single-point levitation system contains rail and electromagnet, we divide the levitation system into a motion system and an electromagnetic system. Due to the regulation time of the motion system is longer than that of the electromagnetic system, the cascade control, whose idea is similar to that of backstepping control, is applied in this paper. Specifically, for the desired gap, the Lyapunov controller and sliding mode controller are designed as Controller I to obtain the desired current, which is regarded as the virtual control, according to which another Lyapunov controller and the standard PID controller as well as the switching controller they form are designed as Controller II to get the real control input, i.e., voltage. Controller I and Controller II constitute the cascade control, whose effectiveness and robustness are verified in numerical sim-

ulations. Compared with the advanced control methods, the controllers designed in this paper are simpler and easy to apply. It should be noted that we used sliding mode controller and fuzzy PID controller to constitute a cascade controller to stabilise maglev systems in [13]. However, the cascade controller in [13] is extremely ineffective when the target position is changed. Thus, we use different controllers to constitute the cascade control instead of the combination in [13], and the combination method is improved to increase the control accuracy and robustness, so that the proposed control strategy in this paper is called improved cascade control.

The main contributions of this paper are as follows: (1) The stable levitation of the nonlinear single-point levitation systems is addressed based on cascade control strategy; (2) The Lyapunov controllers, sliding mode controller, and standard PID controller are designed to constitute the improved cascade control to make the single-point levitation systems levitate in the desired position; (3) The effectiveness and robustness of improved cascade control as well as the influence of control parameters on the control performance are verified and studied in numerical simulations.

The rest of this paper is organized as follows. The dynamical model of single-point levitation systems is constructed and the idea of cascade control is described in Section 2. Controller I and Controller II are designed for motion systems and electromagnet systems respectively, and the design of improved cascade control is presented in Section 3. The improved cascade control is used to stably levitate single-point levitation system to verity the effectiveness and robustness in Section 4. Finally, we conclude this paper and discuss the possible future directions in Section 5.

2. Preliminaries

The levitation frame of a maglev train is structurally decoupled, and each single-point levitation system can be considered independent. Thus, it is universal to study the control of single-point levitation systems. The structures of EMS maglev train and single-point levitation systems are shown in Fig. 1, where the guidance and braking electromagnets as well as the suspension and traction electromagnets are marked in magenta and red, respectively, F is the electromagnetic gravitational force with downward as the positive direction, i is the current in the electromagnetic coil, U is the voltage in the electromagnetic coil, x is the distance between the track and electromagnet, m is the mass of levitated object, and R is the resistance of electromagnetic coil.

We can see from Fig. 1 that EMS maglev trains are composed of several electromagnets (in general, two guidance and braking electromagnets, two suspension and traction electromagnets). Since there is a coupling effect between different electromagnets, i.e., any electromagnet can influence the current and voltage magnitude of the other electromagnets through the magnetic field, the control effect obtained by controlling the currents of four electromagnets through only one gap sensor is not ideal.

By designing a current feedback control loop for each electromagnet separately, the problem of mutual influence between electromagnets can be solved cleverly, which is called mechanical decoupling. After mechanical decoupling, the maglev train levitation system becomes a combination of multiple single-input single-output systems, where each electromagnet is controlled autonomously and does not affect each other. For the EMS maglev train, the levitation system is a mutually coupled system with four inputs and four outputs after mechanical decoupling, i.e., four single-point levitation systems, as can be seen in Fig. 1. For the EMS maglev train levitation system, each electromagnet can control the gap of the levitation system through current feedback, so the single-point levitation system can be regarded as the basic component unit of the maglev train levitation system, such that the control of the maglev train levitation system can

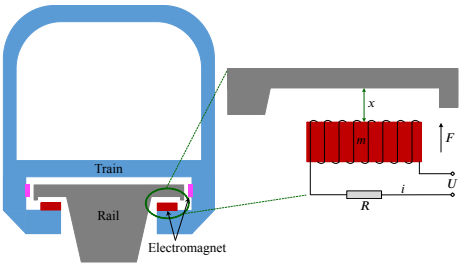

Fig. 1. Schematic diagram of single-point levitation systems for EMS maglev train.

be transformed into the control of single-point levitation systems.

2.1. Dynamical model of single-point levitation systems

In order to obtain a dynamical model of single-point levitation system, the magnetic potential is set to fall uniformly into the air gap and without leakage in this paper, while the electromagnet is considered to have motion only in the vertical direction and no motion in the other directions.

If we let N be the number of turns of the electromagnet coil, S be the effective pole area of the electromagnet, f_m be the magnetic momentum potential, and μ_0 be the vacuum permeability, then the magnetic resistance R_m in the air gap is $R_m = \frac{2x}{\mu_0 S}$. From the magnetic momentum $f_m = Ni$, the magnetic flux in the air gap is $\Phi_l = \frac{f_m}{R_m}$. Thereby, the magnetic induction strength B and magnetic field strength H in the air gap are $B = \frac{\Phi_l}{S}$ and $H = \frac{B}{\mu_0}$, respectively, so that the magnetic field in the air gap can be written as $W = \frac{BHV}{2}$ and the suction force of the electromagnet on the track is $F = \frac{dW}{dx}$. According to Newton's second law, the motion equation of single-point levitation system can be obtained as [13]

$$m\frac{d^2x}{dt^2} = mg + F = mg - \frac{\mu_0 N^2 S}{4}\left(\frac{i}{x}\right)^2 \tag{1}$$

where g is the gravitational acceleration.

On the other hand, the inductance in the coil is $L = \frac{N\Phi_l}{i} = \frac{\mu_0 N^2 S}{2x}$, so the voltage inside the coil is

$$U = Ri + \frac{d}{dt}Li = Ri + \frac{\mu_0 N^2 S}{2x}\dot{i} - \frac{\mu_0 N^2 S i}{2x^2}\dot{x} \tag{2}$$

which is regarded as the electrical equation of the electromagnet. Then, the dynamic equation (1) and the electrical equation (2) of the electromagnet constitute the dynamical model of the single-point levitation system, i.e.,

$$\begin{cases} m\ddot{x} = mg - C\dfrac{i^2}{x^2} \\ U = Ri + \dfrac{2C}{x}\dot{i} - \dfrac{2Ci}{x^2}\dot{x} \end{cases} \tag{3}$$

where $C = \frac{\mu_0 N^2 S}{4}$.

From (3), the single-point levitation system is a nonlinear and open-loop unstable system. Based on (3), the goal of this paper is to design the current i in the electromagnetic coil, which

is regarded as the control input, to make the actual gap x tend to the desired gap x_d, i.e., the single-point levitation system can levitate in the designated position under the designed i.

2.2. Idea of cascade control

In order to achieve the stable levitation, the single-point levitation system is divided into two subsystems, i.e., electromagnetic system and motion system, and the cascade control strategy [13] is used in this paper since the regulation time of the motion system is far longer than that of the electromagnetic system. The diagram of control structure for single-point levitation systems used in this paper is shown in Fig. 2, where x_d is the desired gap value and i_d is the corresponding desired current value. As shown in Fig. 2, we use Controller I to obtain the desired current i_d according to the desired gap x_d and actual gap x first, then apply Controller II to regulate the control voltage U based on the desired current i_d and actual current i to make i tend to i_d such that x tends to x_d, i.e., achieving the stable levitation of the levitation system. Controller I and Controller II constitute the cascade control. The idea of cascade control used in this paper is similar to that of backstepping control, and the current i is regarded as the virtual control. In this paper, we use a Lyapunov controller or a sliding mode controller as the Controller I, while another Lyapunov controller or the standard PID controller or the switching controller they form are regarded as the Controller II. The design of Lyapunov controllers, sliding mode controller and PID controller are shown in Section 3.

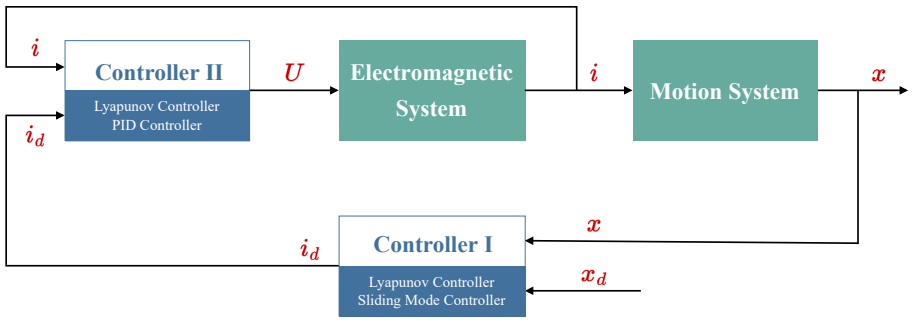

Fig. 2. Diagram of improved cascade control for single-point levitation systems.

3. Design of improved cascade control

From Fig. 2, Controller I is used to obtain the desired current i_d according to the desired gap x_d and actual gap x, i.e., design i to make x tend to x_d, while Controller II is the control voltage U on the electromagnet coil by the actual current i and the target current i_d. We will show the design of Controller I (Lyapunov controller, sliding mode controller) and Controller II (Lyapunov controller, PID controller) in this section.

3.1. Control design for motion systems

3.1.1. Design of Lyapunov controller

The controller designed by the Lyapunov method is not only applicable to time-varying systems, nonlinear systems and even microscopic systems, but also guarantees the stability of the controlled system. Therefore, we use the Lyapunov method to design a controller for electromagnetic systems.

According to Lyapunov stability theorem, for a controlled system described by $\dot{x} = f(x,t)$, the design of Lyapunov controller can follow the following steps: (1) Construct a function $V(x,t)$ that satisfies the conditions of Lyapunov functions, i.e., $V(x,t)$ is continuously derivable of the first order with respect to x and is not less than zero, and $V(x,t) = 0$ only when $x = x_e$, where x_e is the target state; (2) Calculate the first order derivative of $V(x,t)$ with respect to the time t, i.e., $\dot{V}(x,t)$; (3) Design the control law to make $\dot{V}(x,t) \leq 0$ hold and the equality sign holds only at $x = x_e$.

Now, we design a Lyapunov controller as Controller I by applying the above design steps. For the motion system (1), let $x_1 = x$, $x_2 = \dot{x}$, $u = i^2$, then (1) can be rewritten as

$$\begin{cases} \dot{x_1} = x_2 \\ \dot{x_2} = \mathrm{g} - \frac{C}{mx_1^2}u \end{cases} \tag{4}$$

For the motion system (4), the Lyapunov function is designed as

$$V(\boldsymbol{x}) = (\boldsymbol{x} - \boldsymbol{x}_d)^{\mathrm{T}} \boldsymbol{P} (\boldsymbol{x} - \boldsymbol{x}_d) \tag{5}$$

where: $\boldsymbol{x} = [x_1, x_2]^{\mathrm{T}}$ represents the state variable; $\boldsymbol{x}_d = [x_d, 0]^{\mathrm{T}}$ in which x_d is the target gap; $\boldsymbol{P} = \begin{bmatrix} p_{11} & p_{12} \\ p_{21} & p_{22} \end{bmatrix}$ is a positive matrix. From (4) and (5), we have

$$\begin{aligned} \dot{V}(\boldsymbol{x}) =& \dot{\boldsymbol{x}}^{\mathrm{T}} \boldsymbol{P} (\boldsymbol{x} - \boldsymbol{x}_d) + (\boldsymbol{x} - \boldsymbol{x}_d)^{\mathrm{T}} \boldsymbol{P} \dot{\boldsymbol{x}} \\ =& \begin{bmatrix} p_{11}x_2 + p_{21}\left(\mathrm{g} - \frac{C}{mx_1^2}u\right) \\ p_{12}x_2 + p_{22}\left(\mathrm{g} - \frac{C}{mx_1^2}u\right) \end{bmatrix}^{\mathrm{T}} \begin{bmatrix} x_1 - x_d \\ x_2 \end{bmatrix} \\ &+ \begin{bmatrix} p_{11}(x_1 - x_d) + p_{21}x_2 \\ p_{12}(x_1 - x_d) + p_{22}x_2 \end{bmatrix}^{\mathrm{T}} \begin{bmatrix} x_1 - x_d \\ x_2 \end{bmatrix} \\ =& p_{11}x_2(x_1 - x_d) + p_{21}\mathrm{g}(x_1 - x_d) - p_{21}\frac{C(x_1 - x_d)}{mx_1^2}u + p_{12}x_2^2 - p_{22}\frac{Cx_2}{mx_1^2}u \\ &+ p_{22}\mathrm{g}x_2 + p_{11}(x_1 - x_d)^2 + p_{21}x_2(x_1 - x_d) + p_{12}(x_1 - x_d)x_2 + p_{22}x_2^2 \\ =& (p_{11}x_2 + p_{21}\mathrm{g} + p_{11}(x_1 - x_d) + p_{21}x_2 + p_{12}x_2)(x_1 - x_d) \\ &+ (p_{12}x_2 + p_{22}\mathrm{g} + p_{22}x_2)x_2 - \left(p_{21}\frac{C(x_1 - x_d)}{mx_1^2} + p_{22}\frac{Cx_2}{mx_1^2}\right)u \\ =& G(\boldsymbol{x}) - Q(\boldsymbol{x})u \end{aligned} \tag{6}$$

where $G(\boldsymbol{x}) = (p_{11}x_2 + p_{21}\mathrm{g} + p_{11}(x_1 - x_d) + p_{21}x_2 + p_{12}x_2)(x_1 - x_d) + (p_{12}x_2 + p_{22}\mathrm{g} + p_{22}x_2)x_2$, $Q(\boldsymbol{x}) = \frac{Cp_{21}(x_1 - x_d) + Cp_{22}x_2}{mx_1^2}$.

If the control u is designed as $u(\boldsymbol{x}) = \frac{G(\boldsymbol{x})}{Q(\boldsymbol{x})} + k_{l_1} Q(\boldsymbol{x}), k_{l_1} > 0$, i.e., the target current i_d is

$$i_d = \sqrt{\frac{G(\boldsymbol{x})}{Q(\boldsymbol{x})} + k_{l_1} Q(\boldsymbol{x})} \tag{7}$$

then, placing $u(\boldsymbol{x})$ into (6), we have $\dot{V}(\boldsymbol{x}) = -k_{l_1} Q^2(\boldsymbol{x}) \leq 0$.

It is obvious that $Q(\boldsymbol{x}) = 0$ when $\boldsymbol{x} = \boldsymbol{x}_d$. Note that although $Q(\boldsymbol{x})$ is in the denominator of $u(\boldsymbol{x})$ and $Q(\boldsymbol{x}) = 0$ when $\boldsymbol{x} = \boldsymbol{x}_d$, $G(\boldsymbol{x})$ contains higher order infinitesimal terms $(x_1 - x_d)^2$ and $(x_1 - x_d) x_2$ when $\boldsymbol{x} = \boldsymbol{x}_d$, such that

$$\lim_{\boldsymbol{x} \to \boldsymbol{x}_d} u(\boldsymbol{x}) = \frac{p_{21} \mathrm{g} (x_1 - x_d) + p_{22} \mathrm{g} x_2}{p_{21} (x_1 - x_d) + p_{22} x_2} \cdot \frac{m x_1^2}{C} = \frac{\mathrm{g} m}{C} x_d^2 \tag{8}$$

which means $u(\boldsymbol{x})$ is bounded when $\boldsymbol{x} = \boldsymbol{x}_d$. On the other hand, based on LaSalle invariance principle, the gap x tends to the invariant set $\mathcal{R} = \left\{\boldsymbol{x} \in \mathbb{R}^2 : Q(\boldsymbol{x}) = 0\right\}$. We can design $\boldsymbol{P}$ to make $p_{21}(x_1 - x_d) + p_{22} x_2 \neq 0$ hold for $\forall \boldsymbol{x} \in \mathbb{R}^2 \setminus \boldsymbol{x}_d$ such that only $\boldsymbol{x}_d$ is located in the invariant set $\mathcal{R}$, i.e., $\mathcal{R} = \{\boldsymbol{x}_d\}$. For example, the elements in the positive matrix $\boldsymbol{P}$ can be set as

$$\begin{aligned} &p_{11} = p_{22} > 0 \text{ and } p_{11}^2 > p_{12}^2 \\ &p_{21} = p_{12} \begin{cases} > 0, \text{if } (x_1 - x_d) x_2 > 0 \\ < 0, \text{if } (x_1 - x_d) x_2 < 0 \end{cases} \end{aligned} \tag{9}$$

Moreover, in this paper, a normal quadratic function is selected as the Lyapunov function. For the better control performance, logarithmic Lyapunov functions can be considered, e.g., $V(\boldsymbol{x}) = \ln\left(1 + \boldsymbol{x}^{\mathrm{T}} \boldsymbol{P} \boldsymbol{x}\right)$, whose advantages can be found in [14]. The Lyapunov controller designed based on logarithmic Lyapunov functions is similar to that based on quadratic functions, so we ignore it here.

3.1.2. Design of sliding mode controller

Sliding mode control is a nonlinear control method that alters the dynamics of a nonlinear system by applying a discontinuous control signal that forces the system to "slide" along a cross-section of the system's normal behavior. Since the characteristics and parameters of the system only depend on the designed switching hyperplane and have no relationship with external disturbances, the sliding mode control has the advantages of robustness, fast response and simple implementation, and has good control effect on nonlinear systems.

The design of sliding mode controller contains two steps: (1) Design the switching function $s(\boldsymbol{x})$ so that the sliding mode determined by it is asymptotically stable and has good dynamic quality; (2) Design the control law so that the arrival condition is satisfied, and the sliding mode is formed on the sliding mode surface $s(\boldsymbol{x}) = 0$.

For the motion system (4), the linear switching function is selected as the switching function $s(\boldsymbol{x})$ here, i.e., $s(\boldsymbol{x}) = c_1 (x_1 - x_d) + x_2$, where $c_1 > 0$ is the sliding mode surface coefficient. In order to reduce the chattering of sliding mode control, the exponential reaching law is applied, i.e., $\dot{s}(\boldsymbol{x}) = -\varepsilon \mathrm{sgn}(s(\boldsymbol{x})) - k_s s(\boldsymbol{x})$, where, $k_s > 0$; $\mathrm{sgn}(\cdot)$ represents the symbolic function; $\varepsilon > 0$ is the reaching rate of the state variable.

According to the linear switching function and the exponential reaching law, the sliding mode control u can be design as $u(\boldsymbol{x}) = \frac{mx_1^2}{C}(c_1x_2 + \mathrm{g} + \varepsilon\mathrm{sgn}(s(\boldsymbol{x})) + k_s s(\boldsymbol{x}))$, i.e.,

$$i_d = \sqrt{\frac{mx^2}{C}\left(c_1\dot{x} + \mathrm{g} + \varepsilon\mathrm{sgn}\left(c_1\left(x - x_d\right) + \dot{x}\right) + k_s\left(c_1\left(x - x_d\right) + \dot{x}\right)\right)} \tag{10}$$

whose detailed proof can be found in [13].

3.2. Control design for electromagnet systems

3.2.1. Design of Lyapunov controller

For the electromagnet system (2), we can design another Lyapunov controller as Controller II, i.e. the control voltage U on the electromagnet coil.

Following the steps of designing Lyapunov controller, the Lyapunov function for the electromagnet system (2) is constructed as $V(i) = \frac{1}{2}(i - i_d)^2$, whose the first order derivative with respect to the time t is

$$\begin{aligned}\dot{V}(i) &= \dot{i}(i - i_d)\\ &= (i - i_d)\left(\frac{\dot{x}}{x} - \frac{xR}{2C}\right)i + (i - i_d)\frac{x}{2C}\cdot U\end{aligned} \tag{11}$$

In order to make $\dot{V}(i) \leqslant 0$ hold, the control voltage U on the electromagnet coil is designed as $U = \left(R - \frac{2C\dot{x}}{x}\right)i - k_{l_2}(i - i_d)\frac{x}{2C}, k_{l_2} > 0$, which such that $\dot{V}(i) = -k_{l_2}\left((i - i_d)\frac{x}{2C}\right)^2 \leqslant 0$ and $\dot{V}(i) = 0$ only when $i = i_d$.

In fact, according to LaSalle invariance principle, the actual current i can converge to the target current i_d under the control voltage U on the electromagnet coil as shown in (11), while i_d has been shown in (7) or (10).

3.2.2. Design of PID controller

Considering the robustness, the standard PID controller can be applied as Controller II. For the electromagnet system (2), the standard PID controller is described as $U(t) = K_p e(t) + K_i\int_0^t e(\tau)d\tau + K_d\frac{de(t)}{dt}$, where $e(t) = i(t) - i_d$; K_p, K_i, K_d represent the coefficients for the proportional, integral, and derivative terms, respectively, which means the error between the actual current i and the target current i_d is regarded as the input of the PID controller. The key of designing PID controller is to obtain the PID control parameters K_p, K_i, K_d. In this paper, we use the cut and try method to adjust the parameters of PID controller for the electromagnet system (2), which is ignored here. Nevertheless, the PID parameter tuning methods are suggested to be used to obtain better control effects, such as the extended symmetrical optimum method [15].

3.3. Construction of cascade control

We had designed Lyapunov controller and sliding mode controller as Controller I, while another Lyapunov controller and PID controller were design as Controller II. According to the idea of the cascade control strategy, we can obtain four cascade controls for single-point levitation

systems: Lyapunov controller+Lyapunov controller, Lyapunov controller+PID controller, sliding mode controller+Lyapunov controller and sliding mode controller+PID controller, where '+' represents the meaning of combination.

For the designed controllers, Lyapunov controllers can ensure the stability of the controlled system, but the robustness is poor. The standard PID controller has better robustness, but can not ensure the stability, while sliding mode controller can ensure both the stability and robustness of the controlled system. For both the stability and robustness, we use the improved cascade control, i.e., sliding mode controller+PID controller/Lyapunov controller, instead of the four cascade controls mentioned above. In the improved cascade control, we use sliding mode controller as Controller I, while the switching controller consisting of PID controller and Lyapunov controller is used as Controller II. In the switching controller, the switch of PID controller and Lyapunov controller is based on the error between the actual gap x and the target gap x_d, i.e., $|x-x_d|$. Concretely speaking, PID controller is applied when $|x - x_d| \geq \Delta$, otherwise Lyapunov controller is used, where Δ is a positive real number.

Remark 1. *The controllers designed in this section are all in continuous time, while the real applications are expected to be done in discrete time. For practical applications, the designed continuous time controllers can be discretized first and then applied to the actual controlled system. Thus, the design of continuous time controllers is the basis for practical applications. It is worth stating that the discrete time controllers generated by discretizing the continuous time controllers may affect the control performance. Since the discretization of continuous time controllers is not the focus of this paper, we will not discuss it in depth here.*

4. Numerical simulations

In this section, we use the designed cascade control to achieve the stable levitation of the single-point levitation system for EMS maglev trains.

4.1. Stable levitation simulation scenario

In the stable levitation simulations, the initial gap x_0 is set as 7 mm, the desired gap x_d is set as 3 mm. The system parameters R, m, C of the levitation system are set as $R = 3.1\ \Omega$, $m = 14$ Kg and $C = 7.8 \times 10^{-4}$, respectively, which are from [16]. The control parameters in Lyapunov controllers are set as $k_{l_1} = 1$, $k_{l_2} = 2$, $p_{11} = 0.2$ and $p_{12} = \pm 1 \times 10^{-5}$, the control parameters in sliding mode controller are set as $c_1 = 1.5$, $\varepsilon = 0.001$ and $k_s = 10$, while the PID control parameters $K_p = -6$, $K_i = 0.1$, $K_d = 0.1$. Moreover, the gravitational acceleration g is set as $9.8\ \mathrm{m/s^2}$, the initial current i_0 is set as 3 A, and Δ is set as 0.0025. The control parameters in different controllers are determined mainly based on the magnitude of the control amplitude, i.e., the control parameters need to be chosen so that the different controllers as Controller I (or Controller II) have a similar range of control amplitude to avoid errors in the comparison of control performance due to large differences in control amplitude.

According to the control structure diagram in Fig. 2, the controllers (sliding mode controller, Lyapunov controller, and PID controller) designed in Section 3, we built the simulation model in Simulink by using the control parameters mentioned above, which are shown in Fig. 3.

The results of stable levitation under different cascade controls are shown in Fig. 4, where LC, SMC represent Lyapunov controller and sliding mode controller, respectively. From Fig. 4(a),

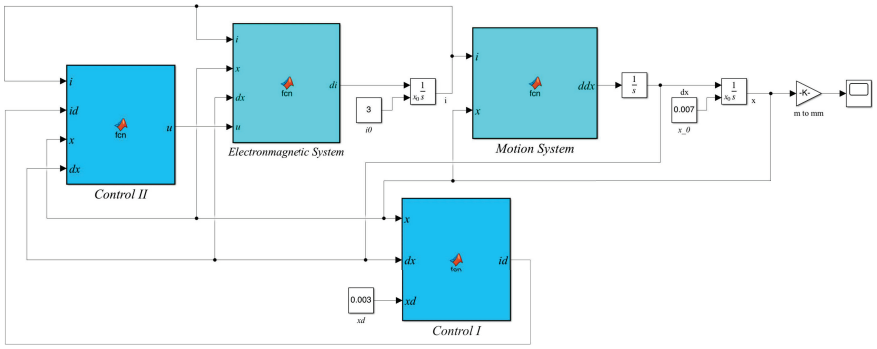

Fig. 3. Simulation model in Simulink.

we can see that the actual gap x tends to the desired gap x_d under the all cascade controls composed by Lyapunov controller, sliding mode controller and PID controller, which verify the effectiveness of the cascade control strategy. Besides, we can also see that the actual gap x can tend to the desired gap x_d faster under SMC+PID/LC than that under LC+LC and SMC+PID. From Fig. 4(b), the steady state error is much smaller under LC+LC and SMC+PID/LC than that under SMC+PID. However, the actual gap under LC+LC occurs oscillations, which affects the convergence rate, thus LC+LC is not an ideal control choice. Considering both convergence rate and steady state error, SMC+PID/LC is recommended. The corresponding cascade controls for the levitation results are shown in Fig. 5.

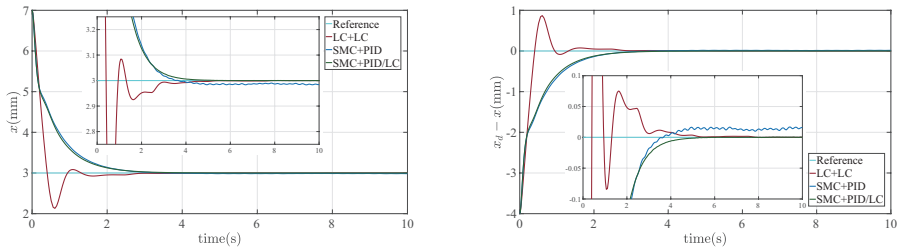

(a) Curves of the actual gap x. (b) Curves of $x_d - x$.

Fig. 4. The results of stable levitation.

Moreover, in order to show the advantages of the control strategy proposed in this paper, we also use sliding mode controller and fuzzy PID controller (the initial control parameters are set as $K_p = 1$, $K_i = 0.1$ and $K_d = 0.1$) in [13] to achieve the stable levitation of single-point levitation systems, and the comparison results are shown in Fig. 6, from which we can see that the SMC+fuzzy PID can make x tend x_d faster in the early stage of stable levitation control (e.g., 0s-0.5s in Fig. 6), but there are big steady-state errors, while almost no steady-state error exists under SMC+PID/LC, which is one of the advantages of the improved cascade control.

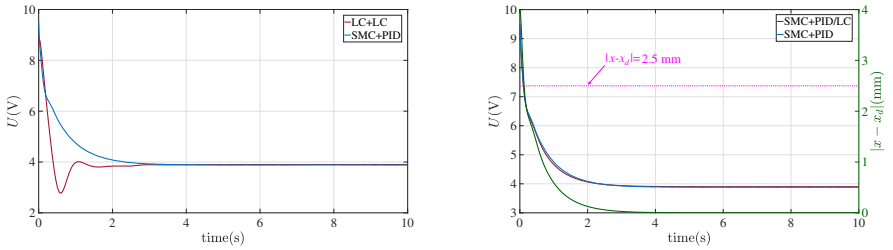

(a) LC+LC vs. SMC+PID (b) SMC+PID vs. SMC+PID/LC

Fig. 5. The cascade controls of stable levitation.

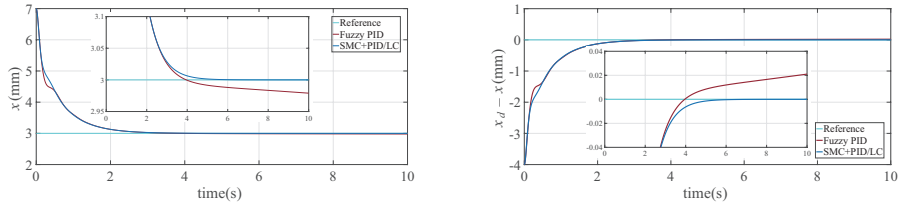

(a) Curves of the actual gap x. (b) Curves of $x_d - x$.

Fig. 6. The comparison of stable levitation under SMC+PID/LC and SMC+Fuzzy PID.

4.2. Robustness simulations

In order to verify the robustness of the cascade control designed in this paper, we perform two robustness simulations, where one simulation is the equivalent mass m of the electromagnet varies from 13.9 Kg to 14.2 Kg, and the other one is to make the desired gap x_d vary from 2.5 mm to 4.0 mm. The cascade control SMC+PID and SMC+PID/LC with $\Delta = 0.00025$ are applied, while the other control parameters are the same as that in the stable levitation simulations.

The results for the varying mass m and the varying desired gap x_d are shown in Figs. 7 and 8, respectively, from which one can see that the proposed control can make x tend to x_d for varying m and x_d, which verify the robustness. Besides, compared with SMC+PID, SMC+PID/LC can make x tend x_d with smaller steady state error, which is consistent with that in subsection 4.1.

In order to study the effect of Δ, we make $\Delta = 0.001$ for the cases of varying m and x_d, and the corresponding results are shown in Fig. 9. One can see from Fig. 9 that the larger Δ may cause larger oscillations and the case of changing x_d is not very sensitive to Δ. Therefore, on balance, we recommend to apply the SMC+PID/LC with smaller Δ for the stable levitation of single-point levitation systems. It should be noted that Δ cannot be taken to zero, otherwise SMC+PID/LC degenerates to SMC+PID, which leads to large steady state errors. The corresponding controls are shown in Fig. 10.

It should be noted that the nonlinear PID control was used to realize the stable levitation of single-point levitation systems in [16]. Compared to the nonlinear PID control, the cascade control designed in this paper has no steady state error, which can be guaranteed theoretically and confirmed by numerical simulations.

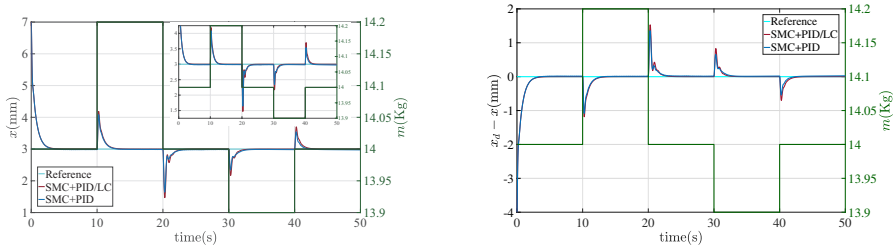

(a) Curves of the actual gap x. (b) Curves of $x_d - x$.

Fig. 7. The results for varying mass m.

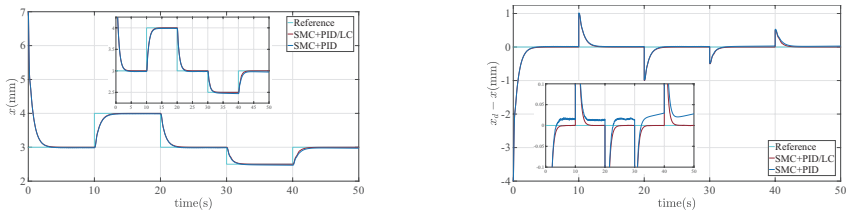

(a) Curves of the actual gap x. (b) Curves of $x_d - x$.

Fig. 8. The results for varying desired gap x_d.

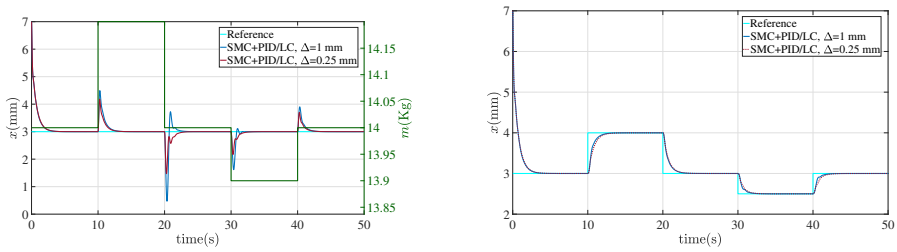

(a) Curves of the actual gap x for varying m. (b) Curves of the actual gap x for varying x_d.

Fig. 9. The results for different Δ.

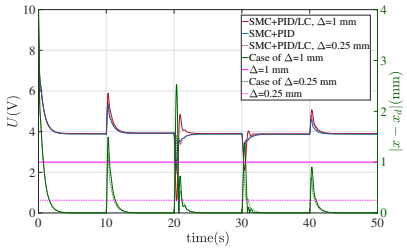

Fig. 10. The controls for different Δ.

5. Conclusions

The stable levitation of the single-point levitation system for EMS maglev train was achieved by applying the improved cascade control in this paper. We divided the single-point levitation system into electromagnetic system and motion system, and the Lyapunov controller, sliding mode controller and PID controller were designed to constitute the cascade control through reasonable collocation to stabilize the single-point levitation system fast and robust, which were also verified in numerical simulations. The further works can be considered as follows: (1) Cooperative control of multi-point levitation system; (2) Robustness analyses in theory instead of in numerical simulations; (3) Ease-of-use enhancement of the designed controllers, such as the application of visualization interfaces [17, 18]; (4) Application of data-driven algorithms [19] or optimization algorithms [20] to help the design of controllers; (5) Simplification and optimization of advanced intelligent controls [21, 22] for application in levitation control.

Acknowledgements. This work was supported by the Natural Science Foundation of Shanxi Province under Grant 202403021211088.

References

[1] Z. SU, J. YANG, Y. PENG and F. PENG, *Simulating active disturbance-resistantcontrol of single-point hybrid magnetic suspension system*, Journal of Railway Science and Engineering **19**(4), 2022, pp. 864–873.

[2] Z. ZHONG, Z. CAI and Y. QI, *Model-free adaptive control for single-degree-of-freedom magnetically levitated system*, Journal of Southwest Jiaotong University **57**(3), 2022, pp. 549–557.

[3] R. WAI and J. LEE, *Robust levitation control for linear maglev rail system using fuzzy neural network*, IEEE Transactions on Control Systems Technology **17**(1), 2009, pp. 4–14.

[4] J. WANG, Q. JIANG, Y. LUO and T. LIU, *Active disturbance rejection generalized predictive control for magnetic levitation system*, Journal of Harbin Institute of Technology **54**(9), 2022, pp. 141–150.

[5] R.WAI and J. LEE, *Backstepping-based levitation control design for linear magnetic levitation rail system*, IET Control Theory & Applications **2**(1), 2008, pp. 72–86.

[6] Y. SUN, J. XU, H. QIANG and G. LIN, *Adaptive neural-fuzzy robust position control scheme for maglev train systems with experimental verification*, IEEE Transactions on Industrial Electronics **66**(11), 2019, pp. 8589–8599.

[7] C. CHEN, J. XU, G. LIN, Y. SUN and X. ZHAO, *Sliding mode bifurcation control based on acceleration feedback correction adaptive compensation for maglev train suspension system with time-varying disturbance*, IEEE Transactions on Transportation Electrification **8**(2), 2022, pp. 2273–2287.

[8] S. JIANG, D. CHEN, T. ZHANG and H. XU, *Nonlinear robust composite levitation control for high-speed EMS trains with input saturation and track irregularities*, IEEE Transactions on Intelligent Transportation Systems **23**(11), 2022, pp. 20323–20336.

[9] Y. SUN, W. LI, J. XU, H. QIANG and C. CHEN, *Nonlinear dynamic modeling and fuzzy sliding-mode controlling of electromagnetic levitation system of low-speed maglev train*, Journal of Vibroengineering **19**(1), 2017, pp. 328–342.

[10] Y. SUN, J. XU, G. LIN, W. JI and L. WANG, *RBF neural network-based supervisor control for maglev vehicles on an elastic track with network time delay*, IEEE Transactions on Industrial Informatics **18**(1), 2022, pp. 509–519.

[11] Y. SUN, J. XU, H. WU, G. LIN and S. MUMTAZ, *Deep learning based semi-supervised control for vertical security of maglev vehicle with guaranteed bounded airgap*, IEEE Transactions on Intelligent Transportation Systems **22**(7), 2021, pp. 4431–4442.

[12] F. ZHAO, K. YOU, S. SONG, W. ZHANG and L. TONG, *Suspension regulation of medium-low-speed maglev trains via deep reinforcement learning*, IEEE Transactions on Artificial Intelligence **2**(4), 2021, pp. 341–351.

[13] J. WEN, J. WU and Y. TIAN, *Levitation control of maglev systems based on cascade control*, 2022 China Automation Congress, Xiamen, China, pp. 4311–4315, 2022.

[14] J. WEN, Y. SHI and X. LU, *Stabilizing a rotary inverted pendulum based on logarithmic Lyapunov function*, Journal of Control Science and Engineering, **2017**, 2017, p. 4091302.

[15] S. PREITL and R.-E. PRECUP, *On the algorithmic design of a class of control systems based on providing the symmetry of open-loop Bode plots*, Scientific Bulletin of UPT, Transactions on Automatic Control and Computer Science **41**(2), 1996, pp. 47–55.

[16] Q. CHEN, X. LI and S. LIU, *Nonlinear PID control for levitation system of maglev train*, Electric Drive for Locomotives **1**, 2014, pp. 52–54.

[17] H. UCGUN, I. OKTEN, U. YUZGEC and M. KESLER, *Test platform and graphical user interface design for vertical take-off and landing drones*, Romanian Journal of Information Science and Technology **25**(3-4), 2022, pp. 350–367.

[18] M. UNGURITU and T. NICHIȚELEA, *Design and assessment of an anti-lock braking system controller*, Romanian Journal of Information Science and Technology **26**(1), 2023, pp. 21–32.

[19] R.-C. ROMAN, R.-E. PRECUP, E.-L. HEDREA, S. PREITL, I. A. ZAMFIRACHE, C.-A. BOJAN-DRAGOS and E. M. PETRIU, *Iterative feedback tuning algorithm for tower crane systems*, Procedia Computer Science **199**, 2022, pp. 157–165.

[20] R.-E. PRECUP, R.-C. DAVID, R.-C. ROMAN, A.-I. SZEDLAK-STINEAN and E. M. PETRIU, *Optimal tuning of interval type-2 fuzzy controllers for nonlinear servo systems using slime mould algorithm*, International Journal of Systems Science **54**(15), 2023, pp. 2941–2956.

[21] Y. FENG, M. WU, L. CHEN, X. CHEN, W. CAO, S. DU and W. PEDRYCZ, *Hybrid intelligent control based on condition identification for combustion process in heating furnace of compact strip production*, IEEE Transactions on Industrial Electronics **69**(3), 2022, pp. 2790–2800.

[22] R.-E. PRECUP, S. PREITL and P. KORONDI, *Fuzzy controllers with maximum sensitivity for servosystems*, IEEE Transactions on Industrial Electronics **54**(3), 2007, pp. 1298–1310.